The Fast Product Multi-Sensor Labeled Multi-Bernoulli Filter

Charlotte Hermann, Martin Herrmann, Thomas Griebel, Michael Buchholz, and Klaus Dietmayer

This paper has been accepted for presentation and publication at the 2023 26th International Conference on Information Fusion (FUSION), June 27 - 30, 2023, Charleston, SC, USA. This is the accepted version of the paper, which has not been fully edited and the layout may differ from the original publication.

Citation information of the original publication:

C. Hermann, M. Herrmann, T. Griebel, M. Buchholz and K. Dietmayer, ”The Fast Product Multi-Sensor Labeled Multi-Bernoulli Filter,” 2023 26th International Conference on Information Fusion (FUSION), Charleston, SC, USA, 2023, pp. 1-8, doi: 10.23919/FUSION52260.2023.10224189.

The Fast Product Multi-Sensor Labeled Multi-Bernoulli Filter

Charlotte Hermann, Martin Herrmann, Thomas Griebel, Michael Buchholz, and Klaus Dietmayer
Institute of Measurement, Control and Microtechnology, Ulm University, Germany
{firstname}.{lastname}@uni-ulm.de

***Abstract*—The multi-sensor Labeled Multi-Bernoulli filter has the challenge of relying on the NP-hard multi-sensor update of the Generalized Labeled Multi-Bernoulli filter. This paper proposes the Fast Product Multi-Sensor Labeled Multi-Bernoulli filter, which is a filter for multi-sensor systems that solves this task by performing computationally simpler single-sensor Labeled Multi-Bernoulli filter updates based on a common prediction for each sensor. These single-sensor updates are then fused using a novel and efficient fusion strategy. Furthermore, the proposed filter is based on the Bayes parallel combination rule and can be seen as an efficient approximation of the multi-sensor Labeled Multi-Bernoulli filter. It enables full parallelization of the update step and benefits from sensor order independence compared to Iterated Corrector implementations. As a result, the robustness is increased, which is important for safety reasons, e.g., in autonomous driving. Our approach is evaluated on simulations, and the results are compared to an Iterated Corrector implementation of the Labeled Multi-Bernoulli filter.**

I. Introduction

The aim of multi-sensor multi-object tracking is to estimate the number of dynamic objects and their trajectories based on measurements from multiple sensors [1]. Furthermore, multiple sensors are commonly used to reduce the uncertainty about the objects' existence and their states [2]. Random Finite Sets (RFSs) [2] provide a useful mathematical basis for multi-object tracking and enable the extension of the Bayes filter to the multi-sensor multi-object case. Well-known filters for the single-sensor case are the Probability Hypothesis Density (PHD) [3] filter, the Cardinalized Probability Hypothesis Density (CPHD) [4] filter, the Generalized Labeled Multi-Bernoulli (GLMB) filter [5], and the Labeled Multi-Bernoulli (LMB) filter [6]. The latter is an efficient approximation of the GLMB filter. For the case of multiple sensors, these approaches can also be extended [7]–[10]. Besides sub-optimal track-to-track fusion approaches [2], [11], centralized tracking architectures offer another way to deal with multiple sensors. Here, the measurements of the sensors are passed to a Fusion Center (FC) with a centralized tracker [12]. Given this architecture, the NP-hard and yet not sufficiently solved track to multi-sensor measurements association is the main problem [13].

There are three main strategies to address this challenge: The Iterated Corrector (IC) approach, sampling-based approaches, and approaches based on the Bayes Parallel Combination Rule (BPCR) [2]. The IC approach is conceptually simple and often used. It applies single-sensor updates for each sensor in turn. However, this is still computationally not feasible, so in practice, approximations are necessary. However, these can decrease the filter's robustness and introduce a dependency on the sensor-order, which has been shown in detail for the IC-GLMB filter in [8]. Moreover, the IC approach can also be applied to the LMB filter allowing for two realizations, the multi-sensor LMB filter with IC-GLMB update [10] or the IC-LMB filter with LMB approximation after each single-sensor update. The latter is an approximation of the multi-sensor LMB filter and has proven to be very useful and efficient for practical applications, such as in our autonomous driving project at Ulm University [14].

The sampling-based Sub-optimal Gibbs Sampling-based GLMB (SO-Gibbs GLMB) filter [8] belongs to the second category of multi-sensor strategies. It provides a better tracking performance than the IC-GLMB filter but sometimes requires more computation time [10]. Further, parallel computation of the single-sensor updates is impossible, as for all filters based on the IC strategy.

Finally, BPCR-based approaches perform a separate update for each sensor and then fuse the results [7], [9], [10]. This has the advantage that only the track to single-sensor measurement associations need to be considered, reducing the computational complexity for each separate update. Additionally, it increases the robustness since the sensor-order becomes irrelevant, and it allows for a parallel computation of the single-sensor updates [15]. There are several implementations already [7], [9], [10], [16], e.g., the Parallel Update multi-sensor LMB (PU-LMB) filter [10], the Product Multi-Sensor GLMB (PM-GLMB) filter [9] and the Product Multi-Sensor LMB (PM-LMB) filter [16]. The latter uses the update of the PM-GLMB filter, which involves the fusion of GLMB densities with many hypotheses, but has the advantage of approximating the fused posterior density as an LMB density. This reduces complexity and, therefore, computation time. Further, the performance of the PM-LMB filter is similar to the PM-GLMB and exceeds that of the IC-LMB filter

Parts of this work were financially supported by the Federal Ministry of Education and Research (BMBF) (project UNICARagil, FKZ 16EMO0290) and by the Federal Ministry for Economic Affairs and Climate Action of Germany within the program "Highly and Fully Automated Driving in Demanding Driving Situations" (project LUKAS, grant number 19A20004F). Parts of this research have been conducted as part of the EVENTS project, which is funded by the European Union, under grant agreement No 101069614. Views and opinions expressed are however those of the author(s) only and do not necessarily reflect those of the European Union or European Commission. Neither the European Union nor the granting authority can be held responsible for them.

and the IC-GLMB filter [16]. The PU-LMB filter [10], in contrast, performs a fusion of LMB densities, which means that only the existence probabilities and the spatial densities of the tracks have to be fused, instead of GLMB hypotheses as for the PM-LMB filter. This offers the advantage of lower computational complexity and also a smaller bandwidth during data transmission. However, the PU-LMB filter cannot resolve the inherent division of the spatial Gaussian Mixture (GM) distributions due to their mixture property [10]. Thus, these are approximated by Gaussians, which comes with a significant information loss and could severely affect the tracking result. All approaches mentioned so far have in common that they need to make a trade-off between tracking performance and computational complexity.

To obtain a computationally more efficient and also robust solution while maintaining good tracking performance, a filter with the following characteristics is required: A computationally efficient fusion based on LMB densities, a sensor-order independent result to obtain robustness, and use of GM distributions to retain as much information as possible.

This paper proposes the Fast Product Multi-Sensor Labeled Multi-Bernoulli (FPM-LMB) filter, the first approach that satisfies all of these requirements. For that, it uses a fusion approach similar to the PM-LMB, made possible by a reformulation of the division of the spatial GM distribution of the PU-LMB filter. This allows in contrast to the PU-LMB filter the exact calculation of the fused spatial density. Furthermore, the direct fusion of the single-sensor updated LMB densities is preserved, which enables a faster implementation than with the PM-LMB filter, since only tracks and not hypotheses need to be considered. Moreover, the fused existence probabilities can be calculated using the same strategy as the PU-LMB filter. This results in a robust filter that performs similarly well to the IC-LMB filter. Its robustness becomes particularly evident in challenging situations, e.g., with unknown occlusions or sensor failures. Such might occur due to security attacks or environmental effects. Moreover, our filter outperforms the others in terms of computational time due to its efficient fusion and a full parallelization of the update step.

This paper is organized as follows: We first summarize our notation and some necessary background in Section II. Then, we propose and discuss the FPM-LMB filter in Section III, followed by a detailed evaluation compared to the IC-LMB filter in Section IV. Conclusions and an outlook on future work are finally given in Section V.

II. Background and Notation

This section briefly introduces our notation. Subsequently, the LMB filter corrector equations for the single-sensor and the multi-sensor case are summarized.

A. Notation

Our notation is based on [9]. Single objects are denoted using small letters, e.g., single-object states are represented by a vector x in some state space $\mathbb{X}$, and single-object measurements are represented by a vector z in some measurement space $\mathbb{Z}$. Multiple objects are modeled on the hyperspace of all finite subsets $\mathcal{F}(\cdot)$ using RFSs [2] and are denoted using capital letters, like the multi-object state RFS X on $\mathcal{F}(\mathbb{X})$ or the multi-object measurement RFS Z on $\mathcal{F}(\mathbb{Z})$. Augmenting the state vectors by a label $\ell \in \mathbb{L}$ yields the labeled single-object state $\boldsymbol{x} = (x, \ell)$ and facilitates the estimation of object trajectories. A labeled multi-object state $\boldsymbol{X} = \{\boldsymbol{x}^{(1)}, \dots, \boldsymbol{x}^{(n)}\}$ for n objects is a labeled RFS on the space $\mathbb{X} \times \mathbb{L}$, where $\mathbb{L}$ is a discrete space. Labeled states and distributions are denoted by boldface letters. The set of track labels of the labeled RFS is extracted by $\mathcal{L}(\boldsymbol{X}) = \{\mathcal{L}(\boldsymbol{x}) : \boldsymbol{x} \in \boldsymbol{X}\}$, given the projection $\mathcal{L}((x, \ell)) = \ell$.

The active sensor is denoted by $s \in \{1, \dots, V\}$, where V denotes the number of used sensors. Moreover, $\theta^{(s)} = I \to \{0, 1, \dots, |Z^{(s)}|\}$ denotes one possible assignement of the measurements $Z^{(s)}$ to the set I of track labels. Unique assignments are ensured by the property $\theta^{(s)}(i) = \theta^{(s)}(i') > 0 \Rightarrow i = i'$. $\theta^{(s)}(i) = 0$ represents the misdetection. The space $\Theta^{(s)}$ contains all possible assignments of measurements to track labels. Besides, the multi-sensor abbreviations $z \triangleq \left(z^{(1)}, \dots, z^{(V)}\right)$, $Z \triangleq \left(Z^{(1)}, \dots, Z^{(V)}\right)$, $\theta \triangleq \left(\theta^{(1)}, \dots, \theta^{(V)}\right)$ and $\Theta \triangleq \Theta^{(1)} \times \cdots \times \Theta^{(V)}$ are used. The generalized Kronecker delta function and the inclusion function supporting sets, vectors, and integers as input arguments are respectively given by

$$\delta_Y(X) \triangleq \begin{cases} 1, & \text{if } X = Y \\ 0, & \text{otherwise} \end{cases} \quad \text{and} \quad 1_Y(X) \triangleq \begin{cases} 1, & \text{if } X \subseteq Y \\ 0, & \text{otherwise} \end{cases}.$$

The multi-object exponential for real-valued functions h is defined by $h^X \triangleq \prod_{x \in X} h(x)$, where $h^{\emptyset} = 1$ by definition. The inner product of two functions $f(x)$ and $g(x)$ is abbreviated by $\langle f, g \rangle \triangleq \int f(x) g(x) dx$. Note that time indices are omitted to simplify notation. Therefore, predicted densities are marked by a '+' subscript. The existence probability of an object is denoted by r. To distinguish RFSs from matrices, the latters are underlined additionally, like the covariance matrix $\underline{P}$. Further, the spatial density of a single object is denoted by p. The multi-object state statistics are described using the multi-object density function π [2].

B. The Labeled Multi-Bernoulli Filter Corrector Equations

The LMB filter [6] is an efficient approximation of the GLMB filter. It uses the expensive GLMB filter update but benefits from approximating the predicted and posterior densities as LMB densities. Given the predicted LMB density $\boldsymbol{\pi}_+(\boldsymbol{X})$ with spatial distributions $p_+^{(\ell)}(x)$ and weights $w_+(I)$, the posterior density of the LMB filter yields

$$\boldsymbol{\pi}\left(\boldsymbol{X} | Z^{(s)}\right) = \left\{\left(r^{(s,\ell)}, p^{(s,\ell)}\right)\right\}_{\ell \in \mathbb{L}^{(s)}}, \tag{1}$$

where the existence probability and the spatial distribution are given by

$$r^{(s,\ell)} = \sum_{\left(I, \theta^{(s)}\right) \in \mathcal{F}\left(\mathbb{L}^{(s)}\right) \times \Theta_I^{(s)}} w^{\left(I, \theta^{(s)}\right)}\left(Z^{(s)}\right) 1_I(\ell), \tag{2a}$$

$$p^{(s,\ell)}(x) = \sum_{(I,\theta^{(s)})\in\mathcal{F}(\mathbb{L}^{(s)})\times\Theta_I^{(s)}} \frac{w^{(I,\theta^{(s)})}\big(Z^{(s)}\big)1_I(\ell)p^{(\theta^{(s)})}\big(x,\ell|Z^{(s)}\big)}{r^{(s,\ell)}} \quad (2b)$$

with

$$w^{(I,\theta^{(s)})}\Big(Z^{(s)}\Big) \propto w_+(I)\Big[\eta_{Z^{(s)}}^{(\theta^{(s)})}\Big]^I, \quad (2c)$$

$$p^{(\theta^{(s)})}\Big(x,\ell|Z^{(s)}\Big) = \frac{p_+^{(\ell)}(x)\psi_{Z^{(s)}}\left(x,\ell;\theta^{(s)}\right)}{\eta_{Z^{(s)}}^{(\theta^{(s)})}(\ell)}, \quad (2d)$$

$$\psi_{Z^{(s)}}\Big(x,\ell;\theta^{(s)}\Big) = \begin{cases} q_D^{(s)}(x,\ell), & \text{if } \theta^{(s)}(\ell)=0 \\ \frac{p_D^{(s)}(x,\ell)g\left(z_{\theta^{(s)}(\ell)}\middle|x,\ell\right)}{\kappa\left(z_{\theta^{(s)}(\ell)}\right)}, & \text{if } \theta^{(s)}(\ell)>0 \end{cases} \quad (2e)$$

$$\eta_{Z^{(s)}}^{(\theta^{(s)})}(\ell) = \Big\langle p_+^{(\ell)}(\cdot), \psi_{Z^{(s)}}\Big(\cdot,\ell;\theta^{(s)}\Big)\Big\rangle. \quad (2f)$$

Here, the posterior weight is denoted by $w^{(I,\theta^{(s)})}\big(Z^{(s)}\big)$. The state dependent detection and misdetection probabilities of track ℓ are denoted $p_D^{(s)}(x,\ell)$ and $q_D^{(s)}(x,\ell)$, respectively. Further, the single-object measurement likelihood for the associated measurement $z_{\theta^{(s)}(\ell)}$ is denoted by $g\big(z_{\theta^{(s)}(\ell)}|x,\ell\big)$, $\eta_{Z^{(s)}}^{(\theta^{(s)})}(\ell)$ denotes the label to single-sensor measurement association likelihood and is calculated using the generalized measurement likelihood $\psi_{Z^{(s)}}\big(x,\ell;\theta^{(s)}\big)$. The clutter process is Poisson distributed and described by the intensity function $\kappa(\cdot)$.

Given that the detection and misdetection probabilities $p_D^{(s)}$ and $q_D^{(s)}$ are state independent and the predicted LMB density is given by $p_+^{(\ell)}(x) = \sum_{j=1}^{J_+^{(\ell)}} \alpha_+^{(\ell,j)}\mathcal{N}(x;\hat{x}_+^{(\ell,j)},\underline{P}^{(\ell,j)})$ with predicted component means $\hat{x}_+^{(\ell,j)}$, covariances $\underline{P}^{(\ell,j)}$, and weights $\alpha_+^{(\ell,j)}$, the LMB filter updated density yields

$$\begin{aligned} &p^{(\theta^{(s)})}\Big(x,\ell|Z^{(s)}\Big) \\ &= \sum_{j=1}^{J_+^{(\ell)}} \tilde{\alpha}^{(s,\ell,j,\theta^{(s)})}\Big(Z^{(s)}\Big)\,\mathcal{N}\Big(x;\hat{x}^{(s,\ell,j,\theta^{(s)})},\underline{P}^{(s,\ell,j)}\Big)\,, \end{aligned} \quad (3)$$

where the weight and the depending normalization constant are given by

$$\tilde{\alpha}^{(s,\ell,j,\theta^{(s)})}\Big(Z^{(s)}\Big) = \frac{\alpha_+^{(\ell,j)}\nu_{Z^{(s)}}^{(s,\ell,j,\theta^{(s)})}}{\eta_{Z^{(s)}}^{(\theta^{(s)})}(\ell)} \quad (4)$$

$$\eta_{Z^{(s)}}^{(\theta^{(s)})}(\ell) = \sum_{\tilde{j}=1}^{\tilde{J}_+^{(\ell)}} \alpha_+^{(\ell,\tilde{j})}\nu_{Z^{(s)}}^{(s,\ell,\tilde{j},\theta^{(s)})}. \quad (5)$$

Like in [16], the mixture component to measurement association likelihood is abbreviated by

$$\nu_{Z^{(s)}}^{(s,\ell,j,\theta^{(s)})} = \begin{cases} q_D^{(s)}, & \text{if } \theta^{(s)}(\ell)=0, \\ \frac{p_D^{(s)}\mathcal{N}\left(z_{\theta^{(s)}(\ell)};z_+^{(s,\ell,j)},\underline{S}^{(s,\ell,j)}\right)}{\kappa\left(z_{\theta^{(s)}(\ell)}\right)}, & \text{if } \theta^{(s)}(\ell)>0. \end{cases} \quad (6)$$

Here, $z_+^{(s,\ell,j)}$ is the predicted measurement and $\underline{S}^{(s,\ell,j)}$ is the corresponding innovation covariance.

Following the same argumentation as in [6] for the LMB filter, the equations for the multi-sensor LMB filter follow in a straight manner. They equal those of the single-sensor case, except for the use of the multi-sensor notation instead of the single-sensor notation, i.e., θ instead of $\theta^{(s)}$, Z instead of $Z^{(s)}$, etc.

III. The Fast Product Multi-Sensor Labeled Multi-Bernoulli Filter

This section focuses on a new Product Multi-Sensor (PM) version of the LMB filter. It proposes the FPM-LMB filter, which applies the BPCR to a reformulation of the fused spatial density of the PU-LMB filter and therefore enables the exact update of spatial densities for GMs. Moreover, it uses the fusion of LMB densities and also the strategy of the PU-LMB filter to update the existence probabilities. In the following, we first discuss the reformulation of the fused spatial density of the PU-LMB filter, then describe the application of the BPCR, which results in the parallel computation of the single sensor spatial densities, and finally derive the FPM-LMB filter.

A. Parallel Calculation of the Spatial Posteriors

To solve the division of GMs in the equation of the PU-LMB filter, we use a strategy similar to that used for the PM-LMB filter to calculate the spatial density. This also makes parallel computation possible. Therefore, a representation is needed that includes the product over the single-sensor measurement likelihood as in the multi-sensor multi-object Bayes filter corrector equations [2].

Proposition 1. *Given the single-sensor posterior spatial distribution in* (2b)*, the spatial density yields*

$$p^{(\ell)}(x) = \frac{1}{\eta_Z^{(\ell)}}\Big(p_+^{(\ell)}(x)\Big)^{1-V}\prod_{s=1}^{V}p^{(s,\ell)}(x) = \frac{p_+^{(\ell)}(x)\hat{\psi}_Z(x,\ell)}{\eta_Z^{(\ell)}} \quad (7a)$$

where the middle part is equivalent to (67) in [10] and

$$\hat{\psi}_Z(x,\ell) = \prod_{s=1}^{V}\sum_{m=0}^{|Z^{(s)}|}\frac{\psi_{Z^{(s)}}(x,\ell;m)}{\eta_{Z^{(s)}}^{(m)}(\ell)}\beta^{(s,\ell,m)}\Big(Z^{(s)}\Big)\,, \quad (7b)$$

$$\eta_Z^{(\ell)} = \Big\langle p_+^{(\ell)}(\cdot),\hat{\psi}_Z(\cdot,\ell)\Big\rangle, \quad (7c)$$

where

$$\beta^{(s,\ell,m)}\Big(Z^{(s)}\Big) = \sum_{(I,\theta^{(s)})\in\mathcal{F}(\mathbb{L}^{(s)})\times\Theta_I^{(s)}}\frac{\delta_{\theta^{(s)}(\ell)}(m)1_I(\ell)w^{(I,\theta^{(s)})}\big(Z^{(s)}\big)}{r^{(s,\ell)}}. \quad (7d)$$

Here $p_+^{(\ell)}$ is the predicted spatial distribution, $\hat{\psi}_Z(x,\ell)$ is the generalized multi-sensor measurement likelihood, which includes the product over the single-sensor measurement association likelihoods, and $\eta_Z^{(\ell)}$ is the multi-sensor normalization constant, which corresponds to the label to multi-sensor measurement association likelihood.

Proof: First a different representation of (2b) is derived. Substitution of (2d) in (2b) and reformulation yields

$$p^{(s,\ell)}(x) = \sum_{\left(I,\theta^{(s)}\right)\in\mathcal{F}\left(\mathbb{L}^{(s)}\right)\times\Theta_I^{(s)}} \frac{1_I(\ell) w^{\left(I,\theta^{(s)}\right)}\left(Z^{(s)}\right)}{r^{(s,\ell)}} \frac{p_+^{(\ell)}(x)\psi_{Z^{(s)}}\left(x,\ell;\theta^{(s)}\right)}{\eta_{Z^{(s)}}^{\left(\theta^{(s)}\right)}(\ell)} \tag{8a}$$

$$= p_+^{(\ell)}(x) \sum_{m=0}^{\left|Z^{(s)}\right|} \frac{\psi_{Z^{(s)}}(x,\ell;m)}{\eta_{Z^{(s)}}^{(m)}(\ell)} \beta^{(s,\ell,m)}\left(Z^{(s)}\right). \tag{8b}$$

The sum in (8a) sums over all GLMB hypotheses with weight $w^{\left(I,\theta^{(s)}\right)}\left(Z^{(s)}\right)$ including a single-sensor posterior spatial density of the track with label ℓ. This results from the update with measurement assignment $\theta^{(s)}(\ell)$ and occurs in several hypotheses. In summary, only one measurement association is considered for a possible single-sensor posterior spatial distribution. Therefore, the summation in (8a) can be reformulated to a summation over the measurements if the Kronecker delta function is used to ensure that only those hypotheses are summed that also contain the appropriate measurement association for the label. This is done in (8b), where the Kronecker delta function in (7d) ensures equality to (8a). Furthermore, the misdetection corresponds to $m = 0$. In other words, a summand in (8b) contains a single-sensor posterior spatial density resulting from the update with the measurement $z_m^{(s)}$. This is then weighted with $\beta^{(s,\ell,m)}\left(Z^{(s)}\right)$, which is the sum of the weights of all hypotheses in which this density occurs.

Substituting of (8b) into the middle part of (7a) yields

$$p^{(\ell)}(x) = \frac{1}{\eta_Z^{(\ell)}} \left(p_+^{(\ell)}(x)\right)^{1-V} \cdot \prod_{s=1}^{V} p_+^{(\ell)}(x) \sum_{m=0}^{\left|Z^{(s)}\right|} \frac{\psi_{Z^{(s)}}(x,\ell;m)}{\eta_{Z^{(s)}}^{(m)}(\ell)} \beta^{(s,\ell,m)}\left(Z^{(s)}\right). \tag{9}$$

Cancelling the predictionresults in

$$p^{(\ell)}(x) = \frac{p_+^{(\ell)}(x)}{\eta_Z^{(\ell)}} \prod_{s=1}^{V} \sum_{m=0}^{\left|Z^{(s)}\right|} \frac{\psi_{Z^{(s)}}(x,\ell;m)}{\eta_{Z^{(s)}}^{(m)}(\ell)} \beta^{(s,\ell,m)}\left(Z^{(s)}\right), \tag{10}$$

which then yields (7b). ∎

Use of GMs for the spatial densities and additional application of the BPCR to (10) comparable to the PM-LMB filter then provides the PM form. Furthermore, it preserves the parallel calculation of the single-sensor posterior spatial distributions shown in the following. This requires the following lemma:

Lemma 1. *Let us assume that the single-sensor update yields a quantity $\zeta_{s,m}$. For this, the prior was associated with the measurement $z_m^{(s)}$ of sensor s, and $\theta^{(s)}$ denotes a single-object track label to measurement association, i.e., not the set-based multi-object association. Then, the following applies:*

$$\sum_{\theta\in\Theta} \prod_{s=1}^{V} \zeta_{s,\theta^{(s)}} = \prod_{s=1}^{V} \sum_{m=0}^{\left|Z^{(s)}\right|} \zeta_{s,m}\,. \tag{11}$$

Proof: Considering the detailed formulation of the left side in (11) yields

$$\begin{aligned}\sum_{\theta\in\Theta} \prod_{s=1}^{V} \zeta_{s,\theta^{(s)}} &= \sum_{\theta^{(1)}\in\Theta^{(1)}} \cdots \sum_{\theta^{(V)}\in\Theta^{(V)}} \zeta_{1,\theta^{(1)}} \cdot \ldots \cdot \zeta_{V,\theta^{(V)}} \\ &= \zeta_{1,0}\cdot\ldots\cdot\zeta_{V,0} + \zeta_{1,0}\cdot\ldots\cdot\zeta_{V-1,0}\cdot\zeta_{V,1} \\ &\quad + \cdots + \zeta_{1,\left|Z^{(1)}\right|}\cdot\ldots\cdot\zeta_{V,\left|Z^{(V)}\right|} = \prod_{s=1}^{V}\sum_{m=0}^{\left|Z^{(s)}\right|}\zeta_{s,m}.\end{aligned}$$

Here, both sides provide all possible measurement permutations of the sensors. ∎

Then the following proposition holds:

Proposition 2. *Given that the detection and misdetection probabilities $p_D^{(s)}$ and $q_D^{(s)}$ are state independent and that the spatial distribution of a predicted object follows a GM distribution as defined in Section II-B, the GM version of the multi-sensor posterior spatial distribution in* (7a) *is given by*

$$p^{(\ell)}(x) = \sum_{j=1}^{J_+^{(\ell)}} \sum_{\theta\in\Theta} \frac{\alpha^{(\ell,j,\theta)}(Z)}{\eta_Z^{(\ell)}} \mathcal{N}\left(x;\hat{x}^{(\ell,j,\theta)},\underline{P}^{(\ell,j,\theta)}\right), \tag{12a}$$

where the respective GM component weights and the normalization constant are given by

$$\alpha^{(\ell,j,\theta)}(Z) = C_Z^{(\ell,j,\theta)} \frac{\prod_{s=1}^{V} \alpha^{\left(s,\ell,j,\theta^{(s)}\right)}\left(Z^{(s)}\right)}{\left(\alpha_+^{(\ell,j)}\right)^{(V-1)}}, \tag{12b}$$

$$\eta_Z^{(\ell)} = \left\langle p_+^{(\ell)}(\cdot), \hat{\psi}_Z(\cdot,\ell)\right\rangle = \sum_{j=1}^{J_+^{(\ell)}} \sum_{\theta\in\Theta} \alpha^{(\ell,j,\theta)}(Z). \tag{12c}$$

Moreover, $C_Z^{(\ell,j,\theta)}$ is a normalization constant and $\alpha^{(s,\ell,j,m)}\left(Z^{(s)}\right)$ is the respective GM component weight of the single-sensor posterior spatial density. Their mean and covariance are obtained by the Information Matrix Fusion (IMF) formulas [12]:

$$\underline{P}^{(\ell,j)} = \left(\left(\underline{P}_+^{(\ell,j)}\right)^{-1} + \sum_{s=1}^{V} I^{(s,\ell,j)}\right)^{-1}, \tag{13}$$

$$x^{(\ell,j,\theta)} = \underline{P}^{(\ell,j)}\left(\left(\underline{P}_+^{(\ell,j)}\right)^{-1} x_+^{(\ell,j)} + \sum_{s=1}^{V} i^{\left(s,\ell,j,\theta^{(s)}\right)}\right), \tag{14}$$

where the information matrix and information vector with measurement matrix $\underline{H}^{(\cdot)}$ and measurement uncertainty matrix $\underline{R}^{(\cdot)}$ are given by

$$I^{(s,\ell,j)} = \left(\underline{H}^{(s,\ell,j)}\right)^T \left(\underline{R}^{(s,\ell,j)}\right)^{-1} \underline{H}^{(s,\ell,j)}, \tag{15}$$

$$i^{(s,\ell,j,\theta^{(s)})} = \left(\underline{H}^{(s,\ell,j)}\right)^T \left(\underline{R}^{(s,\ell,j)}\right)^{-1} z^{(\theta^{(s)})}. \tag{16}$$

Proof: Insertion of (3) into (2b) and using the same reformulation as shown in (8) then yields

$$p^{(s,\ell)}(x) = \sum_{j=1}^{J_+^{(\ell)}} \sum_{m=0}^{|Z^{(s)}|} \alpha^{(s,\ell,j,m)}\left(Z^{(s)}\right) \mathcal{N}\left(x; \hat{x}^{(s,\ell,j,m)}, \underline{P}^{(s,\ell,j)}\right) \tag{17}$$

for the single-sensor posterior density, where

$$\alpha^{(s,\ell,j,m)}\left(Z^{(s)}\right) = \tilde{\alpha}^{(s,\ell,j,m)}\left(Z^{(s)}\right) \beta^{(s,\ell,m)}\left(Z^{(s)}\right). \tag{18}$$

The factor $\beta^{(s,\ell,m)}\left(Z^{(s)}\right)$ is given in (7d) and $\tilde{\alpha}^{(s,\ell,j,m)}\left(Z^{(s)}\right)$ is the respective GM weight of the GLMB posterior density in (3).

Substituting (7b) and the predicted density into (7a) yields

$$p^{(\ell)}(x) = \frac{1}{\eta_Z^{(\ell)}} \left(\sum_{j=1}^{J_+^{(\ell)}} \alpha_+^{(\ell,j)} \mathcal{N}\left(x; \hat{x}_+^{(\ell,j)}, \underline{P}^{(\ell,j)}\right) \cdot \prod_{s=1}^{V} \sum_{m=0}^{|Z^{(s)}|} \frac{\psi_{Z^{(s)}}(x,\ell;m)}{\eta_{Z^{(s)}}^{(m)}(\ell)} \beta^{(s,\ell,m)}\left(Z^{(s)}\right) \right) \tag{19}$$

and $1-V$ fold expansion with the predicted GM component yields

$$p^{(\ell)}(x) = \frac{1}{\eta_Z^{(\ell)}} \left(\sum_{j=1}^{J_+^{(\ell)}} \left(\alpha_+^{(\ell,j)} \mathcal{N}\left(x; \hat{x}_+^{(\ell,j)}, \underline{P}^{(\ell,j)}\right)\right)^{(1-V)} \cdot \prod_{s=1}^{V} \sum_{m=0}^{|Z^{(s)}|} \frac{\alpha_+^{(\ell,j)} \beta^{(s,\ell,m)}\left(Z^{(s)}\right)}{\eta_{Z^{(s)}}^{(m)}(\ell)} \cdot \psi_{Z^{(s)}}(x,\ell;m) \mathcal{N}\left(x; \hat{x}_+^{(\ell,j)}, \underline{P}^{(\ell,j)}\right) \right). \tag{20}$$

Applying the fundamental Gaussian identity [17] to (20) in the same way like in (6) of [15] for the PM-GLMB filter yields

$$p^{(\ell)}(x) = \frac{1}{\eta_Z^{(\ell)}} \sum_{j=1}^{J_+^{(\ell)}} \left(\alpha_+^{(\ell,j)} \mathcal{N}\left(x; \hat{x}_+^{(\ell,j)}, \underline{P}^{(\ell,j)}\right)\right)^{(1-V)} \cdot \prod_{s=1}^{V} \sum_{m=0}^{|Z^{(s)}|} \frac{\alpha_+^{(\ell,j)} \beta^{(s,\ell,m)}\left(Z^{(s)}\right)}{\eta_{Z^{(s)}}^{(m)}(\ell)} \nu_{Z^{(s)}}^{(s,\ell,j,m)} \cdot \mathcal{N}\left(x; \hat{x}^{(s,\ell,j,m)}, \underline{P}^{(s,\ell,j)}\right). \tag{21}$$

Using (4) and (18) then results in

$$p^{(\ell)}(x) = \frac{1}{\eta_Z^{(\ell)}} \sum_{j=1}^{J_+^{(\ell)}} \left(\alpha_+^{(\ell,j)} \mathcal{N}\left(x; \hat{x}_+^{(\ell,j)}, \underline{P}^{(\ell,j)}\right)\right)^{(1-V)} \cdot \prod_{s=1}^{V} \sum_{m=0}^{|Z^{(s)}|} \alpha^{(s,\ell,j,m)}\left(Z^{(s)}\right) \mathcal{N}\left(x; \hat{x}^{(s,\ell,j,m)}, \underline{P}^{(s,\ell,j)}\right). \tag{22}$$

Using (11) and subsequent moving of the $1-V$ fold of the prediction part into the sum then yields

$$p^{(\ell)}(x) = \frac{1}{\eta_Z^{(\ell)}} \sum_{j=1}^{J_+^{(\ell)}} \left(\sum_{\theta\in\Theta} \left(\alpha_+^{(\ell,j)} \mathcal{N}\left(x; \hat{x}_+^{(\ell,j)}, \underline{P}^{(\ell,j)}\right)\right)^{(1-V)} \cdot \prod_{s=1}^{V} \alpha^{(s,\ell,j,\theta^{(s)})}\left(Z^{(s)}\right) \mathcal{N}\left(x; \hat{x}^{(s,\ell,j,\theta^{(s)})}, \underline{P}^{(s,\ell,j)}\right) \right). \tag{23}$$

Subsequent application of the BPCR, as in formula (13) in [15] yields

$$p^{(\ell)}(x) = \frac{1}{\eta_Z^{(\ell)}} \sum_{j=1}^{J_+^{(\ell)}} \sum_{\theta\in\Theta} C_Z^{(\ell,j,\theta)} \mathcal{N}\left(x; \hat{x}^{(\ell,j,\theta)}, \underline{P}^{(\ell,j)}\right) \cdot \left(\alpha_+^{(\ell,j)}\right)^{(1-V)} \prod_{s=1}^{V} \alpha^{\left(s,\ell,j,\theta^{(s)}\right)}\left(Z^{(s)}\right), \tag{24}$$

which equals (12a) when (12b) is substituted. Furthermore this step also enables the use of the IMF formulas (13) and (14) for the means and covariances of the spatial densities. These formulas resemble those of the PM-GLMB filter since the LMB typically retains the spatial density of the GLMB filter [6]. Finally, note that the integration of (24) yields (12c) and that the constant $C_Z^{(\ell,j,\theta)}$ also results from applying the BPCR and can be calculated via (16) in [15]. ■

B. Definition of the Fast Product Multi-Sensor Labeled Multi-Bernoulli Filter and Implementation Details

The FPM-LMB filter combines the proposed exact fusion approach of the spatial densities derived in Section III-A with the fusion of the existence probabilities of the PU-LMB filter [10]. Therefore, the fused existence probability is equal to that in (68) in [10] and is given by

$$r^{(\ell)} = \frac{1_{\mathbb{L}^{(s)}}(\ell) \eta_Z^{(\ell)} (r_+^{(\ell)})^{(1-V)} \prod_{s=1}^{V} r^{(s,\ell)}}{C_p^{(\ell)}} \tag{25}$$

where

$$C_p^{(\ell)} = (1-r_+^{(\ell)})^{(1-V)} \prod_{s=1}^{V} (1-r^{(s,\ell)}) + \eta_Z^{(\ell)} (r_+^{(\ell)})^{(1-V)} \prod_{s=1}^{V} r^{(s,\ell)}. \tag{26}$$

In other words, the sensors calculate the single-sensor LMB posteriors based on a common predicted density, which are subsequently fused using (12a) for the spatial densities and (25) for the existence probabilities.

The advantage of computing the spatial densities as in Section III-A via the IMF equations is that it circumvents the approximation of the spatial distributions, which would be required with the PU-LMB filter due to the division of GMs. Note that the FPM-LMB filter calculates the fused posterior density exactly. In other words, the mean and covariance of

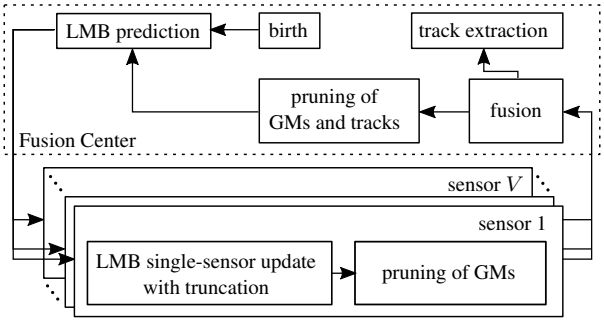

Fig. 1. Schematic overview of the distributed architecture of the FPM-LMB filter. Every single sensor calculates a posterior distribution based on a common prediction. The result is then fused at the FC. Further pruning and truncation are used to achieve a computationally efficient implementation.

the GM components are equivalent to the result of the optimal multi-sensor GLMB update.

With this, the overall structure of the FPM-LMB filter, which belongs to the class of distributed implementations of the centralized estimator, is defined and illustrated in Fig. 1. Specifically, the FC calculates a global predicted LMB density, which also includes the birth of tracks. The result is distributed to the V sensors, which each compute a single-sensor LMB filter update using the single-sensor GLMB filter update step. These are then fused in the FC, which yields the global posterior density that is then used for the next iteration. Furthermore, track extraction is realized by selecting all tracks with an existence probability above a certain threshold.

Since the number of GLMB components grows exponentially with the number of track labels $|\mathbb{L}^{(s)}|$ during the update, truncation is required [6]. This can be done using the Murty ranked assignment algorithm [18], which evaluates only the most significant M components and has already been successfully used in [5]. Furthermore, pruning strategies are applied to the spatial distributions to limit the computational complexity, which also increases with the GM component number of the tracks. Therefore, GM components with a weight below a threshold ϑ_{GM} are removed before and after the fusion and tracks with an existence probability $r^{(\ell)}$ less than a threshold ϑ_r are deleted after the fusion. Furthermore, a hypothesis sampling is used during the LMB-to-GLMB transformation if the cardinality exceeds a certain number N. As already discussed in [15], the constant $C_z^{(\ell,j,\theta)}$ takes a value close to one in theory, but cannot be calculated in a numerically stable way. Thus, it is set to one in the implementation as usual.

IV. Evaluation

The performance of the proposed FPM-LMB filter is evaluated using two different simulation scenarios. The first is based on the linear scenario of [15] and compares the results of the filters for different sensor numbers. The second scenario equals the first but simulates a severe sensor failure to demonstrate the robustness against multiple consecutive sensor failures of our proposed filter. We compare our results to the results of the IC-LMB filter. Both filters share the same LMB filter update implementation and, thus, use the same parameters.

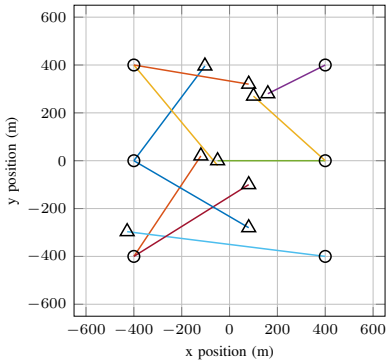

Fig. 2. Ground truth trajectories of the objects in the observed area. The start and end points are marked by circles and triangles, respectively.

A. Simulation Setup

The basic configuration of both scenarios is shown in Fig. 2, where in the 2D surveillance area with $[-800, 800]\,\mathrm{m} \times [-800, 800]\,\mathrm{m}$, a maximum of 10 objects move simultaneously with constant speed. Furthermore, the state vector $x = [p_x, v_x, p_y, v_y]$ contains the position and velocities of the respective track in x and y direction. Both filters use a Constant Velocity (CV) motion model [19] with sampling time $T = 1\,\mathrm{s}$, standard deviation of the discrete white noise sequence $\sigma_a = 0.2\,\mathrm{m\,s^{-2}}$, and survival probability $p_S = 0.98$ in the prediction. Newly born tracks can only arise at static birth regions $\left[p_{B,x}^{(i)}, p_{B,y}^{(i)}\right]$, which are marked by circles in Fig. 2 and modeled by an LMB density with $\boldsymbol{\pi}_B \left\{r_B, p_B^{(i)}\right\}_{i=1}^{6}$, where $r_B = 0.05$ and $p_B^{(i)} = \mathcal{N}\left(x; x_B^{(i)}, \underline{Q}_B\right)$. The state vector of a birth track is given by $x_B^{(i)} = \left[p_{B,x}^{(i)}, 0, p_{B,y}^{(i)}, 0\right]$ and the corresponding covariance is $\underline{Q}_B = \mathrm{diag}([15\,\mathrm{m}, 5\,\mathrm{m\,s^{-2}}, 15\mathrm{m}, 5\,\mathrm{m\,s^{-2}}])^2$. Moreover, six synchronous omnidirectional sensors with constant detection probability p_D perform the detection of the objects. These sensors deliver positional measurements with measurement noise covariance $\underline{R} = \mathrm{diag}([0.36\,\mathrm{m}^2, 0.36\,\mathrm{m}^2])$. The clutter of each sensor follows a Poisson distribution with a mean number of $\lambda_c = 7$ measurements, which are uniformly distributed over the observed area. The truncation parameter is set to $M = 3000$, and the pruning parameters are set to $\vartheta_r = 0.01$ and $\vartheta_{GM} = 0.001$. Track extraction is done by selecting all tracks with existence probability $r^{(\ell)} > 0.5$. Hypotheses sampling during the transformation from LMB-to-GLMB is done for cardinalities above $N = 8$. For the IC-LMB filter, pruning of tracks and GM components takes place after each single-sensor update. The results of both scenarios are averaged over 100 Monte Carlo (MC) runs each and evaluated using the Optimal Sub-pattern Assignment metric (OSPA) and the OSPA-on-OSPA (OSPA$^{(2)}$) metrics [20], with OSPA order $p = 1$, cut-off $c = 2$ and window length $w = 20$.

B. Linear Scenario

This scenario compares the results of the two filters for two cases, one using all six sensors and the other using only two sensors. A detection probability of $p_D = 0.67$ was chosen.

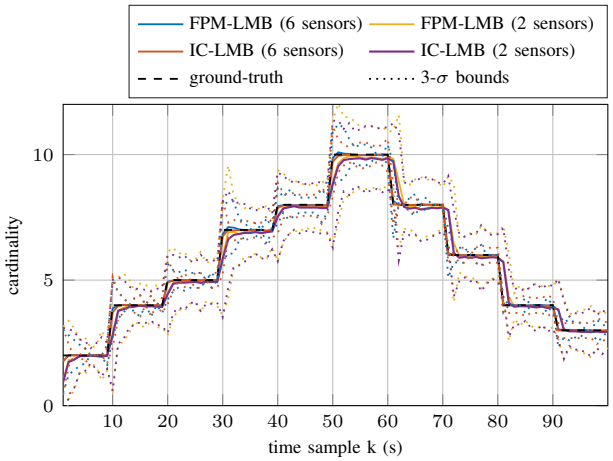

Fig. 3. Cardinality estimation of the FPM-LMB filter and the IC-LMB filter for the Linear Scenario averaged over 100 simulation runs.

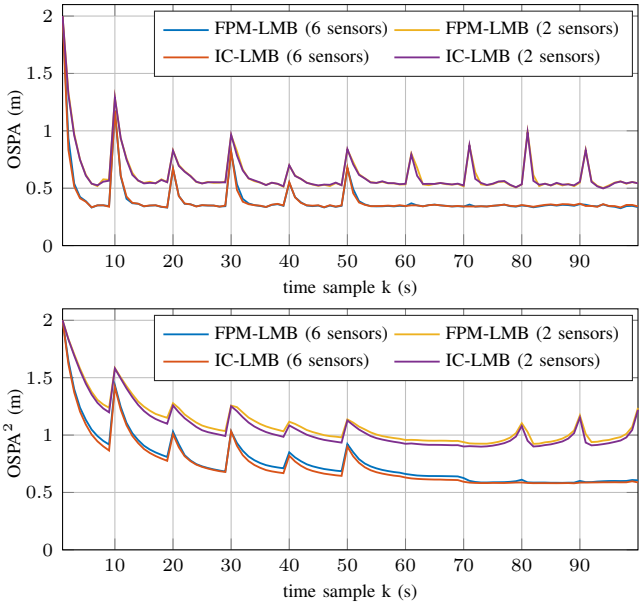

Fig. 4. OSPA and OSPA$^{(2)}$ error of both filters for the Linear Scenario averaged over 100 simulation runs.

Overall, both filters perform similarly well for both cases, as can be seen in the cardinality plot in Fig. 3 and the OSPA error plots in Fig. 4. At the latter, it is also obvious that the estimation of the object state is also similar. In the case of two sensors, the result of both filters is worse overall due to the lower measurement information, which is consistent with theory. However, the FPM-LMB filter sometimes tends to overestimate the cardinality when tracks are born, while the IC-LMB filter always tends to underestimate the cardinality in this case. The overestimation of the FPM-LMB filter is caused by the static birth model. This creates a track at each timestep for all places of birth. Due to the slow velocity of the objects, measurements can sometimes be meaningfully associated with several tracks, especially close to the birth regions. Then, the FPM-LMB filter can keep track of multiple concurrent tracks,

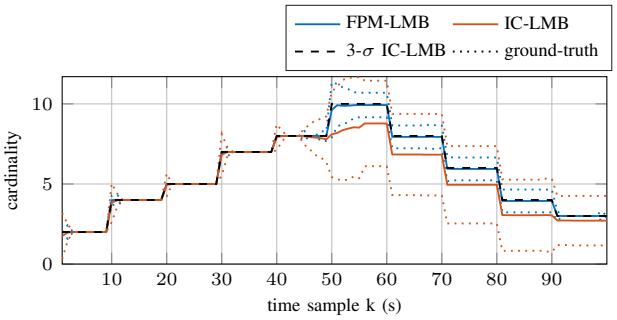

Fig. 5. Cardinality estimation of the FPM-LMB filter and the IC-LMB filter for the Linear Scenario with Severe Sensor Failure averaged over 100 simulation runs.

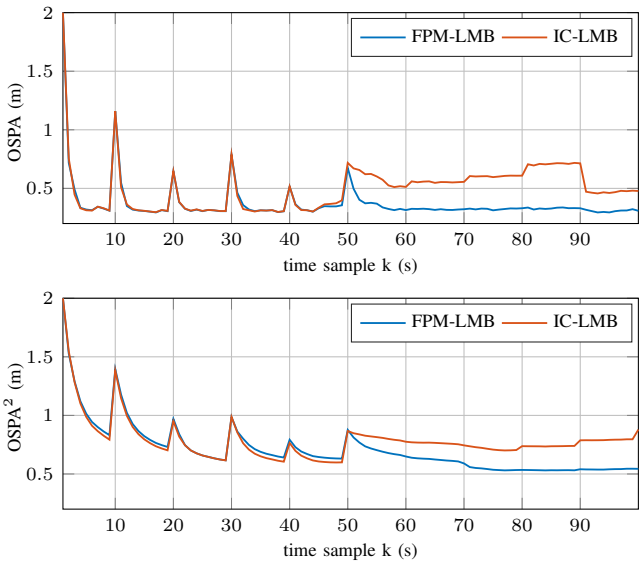

Fig. 6. OSPA and OSPA$^{(2)}$ error of both filters for the Linear Scenario with Severe Sensor Failure averaged over 100 simulation runs.

while only one prevails in the IC-LMB filter, in contrast. Thus, the PM-LMB filter shows slightly more label switches using the static birth model, which reflects in the minimally worse OSPA$^{(2)}$ metric. Moreover, the FPM-LMB filter tends to detect disappearing tracks little later than the IC-LMB filter.

C. Linear Scenario with Severe Sensor Failure

Now we want to investigate the behavior in case of several sensor failures, e.g., caused by security attacks, a (temporary) sensor failure, or a failure of the communication channel. Therefore, in this scenario, two of the six sensors from the linear scenario do not provide any detections in the period $44 < k < 56$. For the IC-LMB filter, this corresponds to the failure of the first two sensors in this time range. In addition, to emphasize the different behavior of the two filters in this case, a higher detection probability of $p_D = 0.9$ was chosen in this scenario. The results up to time step 44 are similar to those of the linear scenario for the same arguments given there. However, the differences between the filters are even smaller here due to the higher detection probability.

TABLE I
COMPUTATION TIME SAVINGS OF THE FPM-LMB FILTER RELATIVE TO THE IC-LMB FILTER

Scenario	Two sensors	Six sensors
Linear Scenario	-22.33%	-41.89%
Linear Scenario with Sensor Failure	—	-43.41%

Hence, we focus on the sensor failures in the following. The cardinality plot in Fig. 5 shows the behavior of the filters as expected in the introduction and Section III. Due to the iterative update and pruning after each single-sensor update, the IC-LMB filter tends to assume that tracks have already disappeared or are not born at all. Therefore, it significantly underestimates the cardinality from the beginning of the sensors' failure compared to the FPM-LMB filter. Due to the static birth model, once deleted, tracks cannot reappear even if there are matching measurements, which is why the cardinality estimate remains worse even after the end of the sensor failure. The FPM-LMB filter, on the other hand, shows the expected robust behavior, since it considers all sensor measurements simultaneously and does not make any premature decisions. This behavior can also be seen in the plots of the OSPA and OSPA$^{(2)}$ error in Fig. 6, which show a lower error for the FPM-LMB filter from the moment the two sensors fail.

D. Computation Time

To show the efficiency of the fusion, the percentage deviations of the calculation time of the IC-LMB filter compared to the FPM-LMB filter are listed in Table I for both simulated scenarios. Both filters share the same code for birth, prediction, update, and track extraction. The main difference is in the update, which is iteratively executed by the IC-LMB filter and parallelly calculated with subsequent fusion in the FPM-LMB filter. In the latter case, the computation time of the parallel sensor update is equal to the computation time of the slowest single-sensor update, independent of the number of sensors. We performed all simulations on an AMD Ryzen 7 3800X processor. The results in Table I show that our filter outperforms the IC-LMB filter with respect to execution time. For a higher number of sensors, this computing time saving compared to the IC-LMB filter and, thus, efficiency gain even increases.

V. CONCLUSION

In this paper, we derived the FPM-LMB filter that performs similarly to the IC-LMB filter with respect to tracking results. However, in more challenging scenarios with sensor failures, the proposed FPM-LMB shows much higher robustness and independence from sensor-order compared to the IC-LMB filter. Furthermore, its update computation time is independent of the number of sensors, which, together with the efficient fusion, results in a lower computation time compared to the IC-LMB filter. This has been demonstrated in detailed evaluations. Moreover, the new filter offers the advantage of a fusion of LMB densities using GMs, where mean and covariance of the GM components correspond to the result of the optimal multi-sensor GLMB update. At the same time, the estimation of the existence probability is the same as in the PU-LMB filter, so the FPM-LMB filter can be considered as its extension. For easier application, we also provided details for computationally efficient implementation.

In future work, we aim to extend our filter by dynamic birth models to reduce label-switching. Finally, with these extensions, we plan to evaluate the filter on real-world applications.

REFERENCES

[1] Y. Bar-Shalom and T. E. Fortmann, *Tracking and Data Association*. Academic Press, Inc., New York, 1988.

[2] R. P. S. Mahler, *Statistical Multisource-Multitarget Information Fusion*. Artech House, Inc., Norwood, 2007.

[3] ——, "Multitarget bayes filtering via first-order multitarget moments," *IEEE Transactions on Aerospace and Electronic Systems*, vol. 39, no. 4, pp. 1152–1178, 2003.

[4] ——, "PHD filters of higher order in target number," *IEEE Transactions on Aerospace and Electronic Systems*, vol. 43, no. 4, pp. 1523–1543, 2007.

[5] B.-T. Vo and B.-N. Vo, "Labeled random finite sets and multi-object conjugate priors," *IEEE Transactions on Signal Processing*, vol. 61, no. 13, pp. 3460–3475, 2013.

[6] S. Reuter, B.-T. Vo, B.-N. Vo, and K. Dietmayer, "The labeled multi-Bernoulli filter," *IEEE Transactions on Signal Processing*, vol. 62, no. 12, pp. 3246–3260, 2014.

[7] R. P. S. Mahler, "Approximate multisensor CPHD and PHD filters," in *Proc. 13th International Conference on Information Fusion*, 2010, pp. 1–8.

[8] B. N. Vo, B. T. Vo, and M. Beard, "Multi-sensor multi-object tracking with the generalized labeled multi-Bernoulli filter," *IEEE Transactions on Signal Processing*, vol. 67, no. 23, pp. 5952–5967, 2019.

[9] M. Herrmann, C. Hermann, and M. Buchholz, "Distributed implementation of the centralized generalized labeled multi-Bernoulli filter," *IEEE Transactions on Signal Processing*, vol. 69, pp. 5159–5174, 2021.

[10] S. C. Robertson, C. E. van Daalen, and J. A. du Preez, "Efficient approximations of the multi-sensor labelled multi-Bernoulli filter," *Signal Processing*, vol. 199, pp. 1–30, 2022.

[11] M. E. Liggins, C. Y. Chong, I. Kadar, M. G. Alford, V. Vannicola, and S. Thomopoulos, "Distributed fusion architectures and algorithms for target tracking," *Proceedings of the IEEE*, vol. 85, no. 1, pp. 95–106, 1997.

[12] Y. Bar-Shalom, *Tracking and Data Fusion: A Handbook of Algorithms*. YBS Publishing, Storrs, Conn, 2011.

[13] A. Buonviri, M. York, K. Legrand, and J. Meub, "Survey of challenges in labeled random finite set distributed multi-sensor multi-object tracking," *IEEE Aerospace Conference Proceedings*, 2019.

[14] F. Kunz, D. Nuss, J. Wiest, H. Deusch, S. Reuter, F. Gritschneder, A. Scheel, M. Stubler, M. Bach, P. Hatzelmann, C. Wild, and K. Dietmayer, "Autonomous driving at Ulm University: A modular, robust, and sensor-independent fusion approach," *IEEE Intelligent Vehicles Symposium, Proceedings*, vol. 2015-Augus, pp. 666–673, 2015.

[15] M. Herrmann, T. Luchterhand, C. Hermann, T. Wodtko, J. Strohbeck, and M. Buchholz, "Notes on the product multi-sensor generalized labeled multi-Bernoulli filter and its implementation," *25st International Conference on Information Fusion*, no. 768953, 2022.

[16] M. Herrmann, T. Luchterhand, C. Hermann, and M. Buchholz, "The product multi-sensor labeled multi-Bernoulli filter," *26st International Conference on Information Fusion*, to be published, 2023.

[17] Y. C. Ho and R. C. Lee, "A Bayesian approach to problems in stochastic estimation and control," *IEEE Transactions on Automatic Control*, vol. 9, no. 4, pp. 333–339, 1964.

[18] K. Murty, "An algorithm for ranking all the assignments in order of increasing cost," *Operations Research*, vol. 16, no. 3, pp. 682–687, 1968.

[19] Y. Bar-Shalom, X.-R. Li, and T. Kirubarajan, *Estimation with Applications to Tracking and Navigation*. John Wiley & Sons, Inc., 2001.

[20] M. Beard, B. T. Vo, and B.-N. Vo, "OSPA(2): Using the OSPA metric to evaluate multi-target tracking performance," in *IEEE International Conference on Control, Automation and Information Sciences*, 2017.